Improvement of single photon emission from InGaN QDs embedded in porous micropillars

H.P. Springbett[1,2], K. Gao (高亢)[2], J. Jarman[1], T. Zhu[1], M. Holmes[2,3*], Y. Arakawa[2,3], R.A. Oliver[1]

1. Department of Materials Science and Metallurgy, 27 Charles Babbage Road, Cambridge, CB3 0FS, United Kingdom
2. Institute of Industrial Science (IIS), The University of Tokyo, 4-6-1 Komaba, Meguro-ku, Tokyo, 153-8505, Japan
3. Institute for Nano Quantum Information Electronics (NanoQuine), The University of Tokyo, 4-6-1 Komaba, Meguro-ku, Tokyo, 153-8505, Japan

[*] Email: holmes@iis.u-tokyo.ac.jp

Abstract

In many InGaN/GaN single photon emitting structures, significant contamination of the single photon stream by background emission is observed. Here, utilizing InGaN/GaN quantum dots incorporated in mesoporous distributed Bragg reflectors within micropillars, we demonstrate methods for the reduction of this contamination. Using the resulting devices, autocorrelation measurements were performed using an HBT set-up and thus we report a working quantum dot device in the III-nitride system utilizing mesoporous DBRs. Uncorrected $g^{(2)}(0)$ autocorrelation values are shown to be significantly improved when excited with a laser at longer wavelengths and lower powers. Through this optimization, we report a $g^{(2)}(0)$ value from a blue-emitting InGaN/GaN quantum dot of 0.126 ± 0.003 without any form of background correction.

Many applications require the on-demand emission of one, and only one photon, such as quantum cryptography [1,2], linear optical quantum computing [3], and true random number generation [4]. Single photon emission has been demonstrated from a range of quantum emitters such as trapped ions [5], single molecules [6], atoms [7], diamond vacancy-centres [8], and semiconductor quantum dots (QDs) [9]. QD single photon emitters are of particular interest as they boast good stability, narrow spectral emission line-width, rapid radiative recombination rates, and the ability to be integrated in, and coupled to, optical cavities [10].

Over recent years the III-nitride semiconductor materials system has enjoyed great success in LED and laser structures [11], but it also displays many advantages for use as single photon sources. The access to visible wavelengths it provides is particularly beneficial as it is this region where non-cryogenic ultrafast single photon detectors display greatest sensitivity, and so the size of transmitter and receiver optics for free-space cryptography could be reduced [12]. Furthermore, comparably high-temperature emission has been reported up to 280 K for InGaN-GaN QDs [13,14] and 350 K for GaN-AlGaN QDs [15], while GaAs dots typically emit only at cryogenic temperatures [16]. This shows the potential to achieve efficient single photon emission at room temperature, or at least at temperatures accessible by on-chip Peltier cooling, which eliminates the need for expensive and cumbersome cryogenic cooling. Distributed Bragg Reflectors, consisting of alternating layers of high and low refractive index materials, are a potentially important component in moving towards a working commercial quantum device. Back reflector structures can be used to improve the extraction efficiency of photons from a quantum dot [17], and ultimately cavities can also be formed to achieve enhancement of the emission [18]. Traditionally these DBR structures have consisted of epitaxial layers of nitride alloys with differing refractive indices. However this method is limited, as none of the material choices are without significant drawbacks; the composition of $Al_xGa_{1-x}N$ required to achieve a significant refractive index contrast displays a large lattice mismatch to c-plane GaN, which can lead to dislocations and cracks [19,20]. Alternatively, $Al_xIn_{1-x}N$ can be lattice-matched to c-plane GaN yet exhibits such a small refractive index contrast that a large number of layers is required, which coupled with an extremely slow growth rate, leads to long growth times [21,22]. Additionally, the available refractive index contrast under lattice-matched conditions is limited. On the other hand, the recently developed mesoporous DBRs consist of alternating layers of homogenous and mesoporous GaN, and are thus lattice-matched. The effective refractive index of the mesoporous layers can be calculated as a weighted average of the refractive indices of air and GaN, and so a high refractive index contrast is possible for highly porous structures. Furthermore, this recently developed fabrication method boasts a fast growth rate and facile fabrication method [23].

Our QD samples were grown by metal-organic vapour phase epitaxy in a 6 x 2 inch Thomas Swan close-coupled showerhead reactor on c-plane sapphire. We utilise the recently developed wafer-scale fabrication of III-nitride mesoporous DBR (MP-GaN DBR) using a facile electrochemical porosification of epitaxially grown lattice-matched alternating Si-doped (~2×10^{19} cm^{-3}) and undoped GaN layers [23]. The InGaN QDs were grown using a modified droplet epitaxy method [24,25], which are located in the centre of a 200 nm intrinsic GaN layer between the top and bottom MP-GaN DBRs. After sample epitaxy, 10 pairs of top and 10 pairs of bottom GaN/MP-GaN (56 nm and 47 nm thick, respectively) DBRs were formed in a simple one-step electrochemical etching without any extra processing steps. Upon the application of a bias to the sample in an Oxalic acid-based electrolyte, the Si-doped nGaN layers were selectively porosified, which proceeded both vertically and laterally [23]. After electrochemical porosification and formation of the MP-GaN DBRs, porous micropillars were made by first drop casting silica microspheres followed by inductively coupled plasma reactive-ion dry etching to a depth of ~1.5 µm. The mesoporous DBR structure and the resulting porous pillar structures can be seen in Fig.s 1 a) and b).

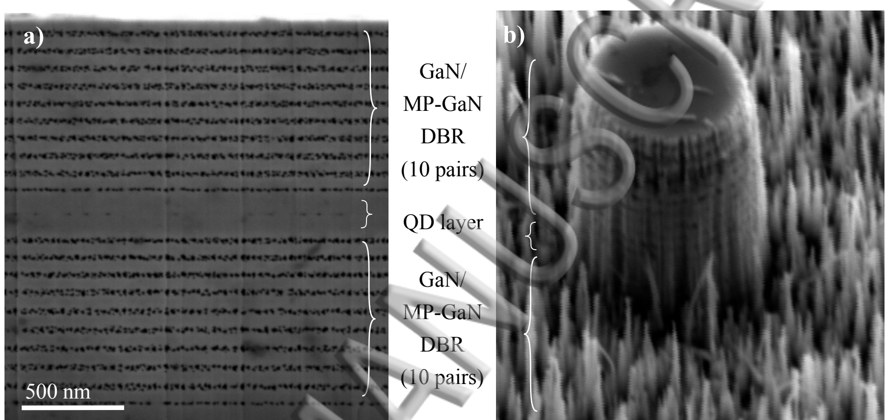

Figure 1. a) SEM image of a cross section of the mesoporous DBR. Ten pairs of mesoporous-GaN/GaN layers positioned above the QD layer, and ten pairs below. b) SEM image of the etched micropillar.

Optical measurements were performed on porous samples with and without micropillars using microphotoluminescence (µPL) spectroscopy. The samples were held in a cryostat at a nominal temperature of 5.6 K, and optical excitation was achieved using a frequency doubled femtosecond-pulse tuneable Ti:Al_2O_3 laser tuned to 350 nm, 375 nm and 400 nm. The emission was collected using a 50x magnification objective lens (N.A. 0.4) and analysed using a 300 mm spectrometer with a 1200 lines mm^{-1} grating and a liquid nitrogen-cooled charge couple device (CCD) camera. Autocorrelation measurements were made using a Hanbury Brown and Twiss (HBT) configuration by passing the signal though a 50/50 beam splitter to two photo-multiplier tubes (PMTs).

Figure 2 a) and c) shows emission spectra measured from areas of non-pillared and pillared samples, respectively (for both cases the samples were measured under excitation at 375 nm with a power of 4.56 µW). Although sharp peaks from QD emission can be observed in both samples, it can be seen that the micropillar structures have allowed for a significant reduction in collected background emission. The reason for this is likely to be two-fold: firstly, the reduction in the material volume reduces the area of quantum well (which is the source of the background emission). Secondly, the introduction of increased surface area will allow carriers within the quantum well to diffuse to the pillar surface, where they can undergo non-radiative recombination [26]. These effects will cause a reduction in the emission intensity of the quantum well relative to the quantum dot. Autocorrelation measurements were performed on the emission peaks in the spectra (see figure 2 b) and d), respectively), and while no discernible anti-bunching can be observed from the non-pillared sample, a $g^{(2)}(0)$ value of 0.307 ± 0.005 is observed from the pillared sample. This is below the limit of 0.5 required to conclusively demonstrate single photon emission [16], and is therefore evidence of the presence of a single quantum emitter in the pillar.

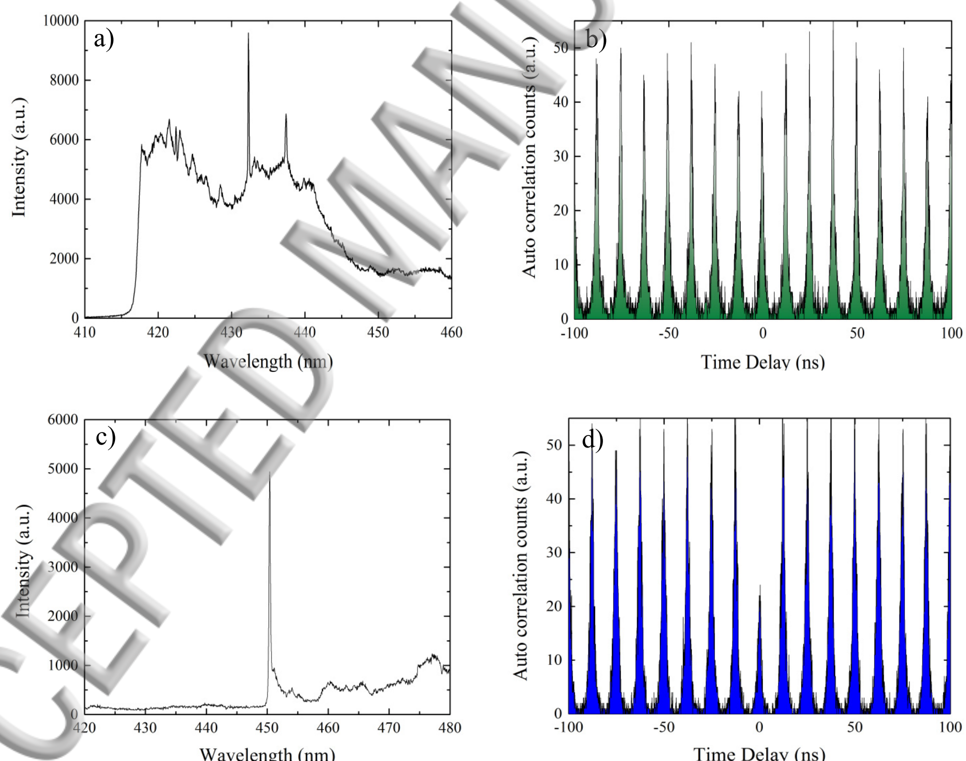

Figure 2. a) Spectrum and b) autocorrelation histogram from the non-pillared porous DBR sample excited by a 375 nm pulsed laser at 4.56 µW. c) Spectrum and d) autocorrelation histogram from the pillared DBR sample. The non-pillared DBR sample shows no discernible anti-bunching, while the pillared sample exhibits a $g^{(2)}(0)$ of 0.307 ± 0.005.

In order to further improve the purity with which the single photon emission could be extracted, the pillared sample was probed with varying excitation conditions. Pulsed laser sources of wavelength 350 nm, 375 nm, and 400 nm (second order harmonics of a tuneable Ti:Sapphire laser at 80MHz) were used to excite the sample; and in each case measurements were taken at a range of laser powers. Figure 3 shows a plot of all the $g^{(2)}(0)$ values recorded in this series, alongside the spectra and autocorrelation histograms corresponding to the lowest and largest $g^{(2)}(0)$ values. We see that by reducing both the excitation power and energy, the emission from the QD can be extracted with less background contamination, and, hence, increased purity. The lowest $g^{(2)}(0)$ value of 0.126 ± 0.003 was obtained using excitation at 400 nm at a power of 0.8 μW. By tuning the excitation energy below the GaN bandgap (λ >~355nm), we selectively excite carriers only in the active region, which leads to a reduced background. By further tuning the excitation wavelength to 400nm, where the density of states in the InGaN layer is lower, we are able to further reduce the overall carrier density, and achieve a cleaner emission spectrum with less background contamination (a similar effect is obtained by reducing the excitation power). Together these effects enable the isolation of the single photons from the QD with increased purity. We note that the values of $g^{(2)}(0)$ that we present are the measured raw values, and are uncorrected in any way. They thus represent the true purity with which the single photons are emitted, and can be isolated and measured with our system.

This increased purity comes with the caveat of reduced emission intensity, although we note that the photon detection rate was still as large as 9000 cps on the PMT detectors, corresponding to a collection rate of 10^5 photons per second by the objective lens [NA 0.4]. (For 350 nm excitation at 2.4 μW we achieve a $g^{(2)}(0)$ value of less than 0.5 and count rates as high as 3.6×10^4 cps on the PMT detectors, corresponding to a collection rate of 5×10^5 photons per second). This rate is currently limited by the extent to which we can collect all emitted photons with our NA 0.4 objective, and the internal efficiencies related to the dot excitation and emission processes, including any non-radiative decay. The overall efficiency between laser excitation (80MHz) and collection is ~0.1%, and if this could be improved to 100%, we could then expect an even further improvement of the emission rate (up to >1GHz) by using a faster excitation rate, and non-polar QDs [25], cubic [27] or smaller QDs [28], which would be expected to exhibit faster emission lifetimes.

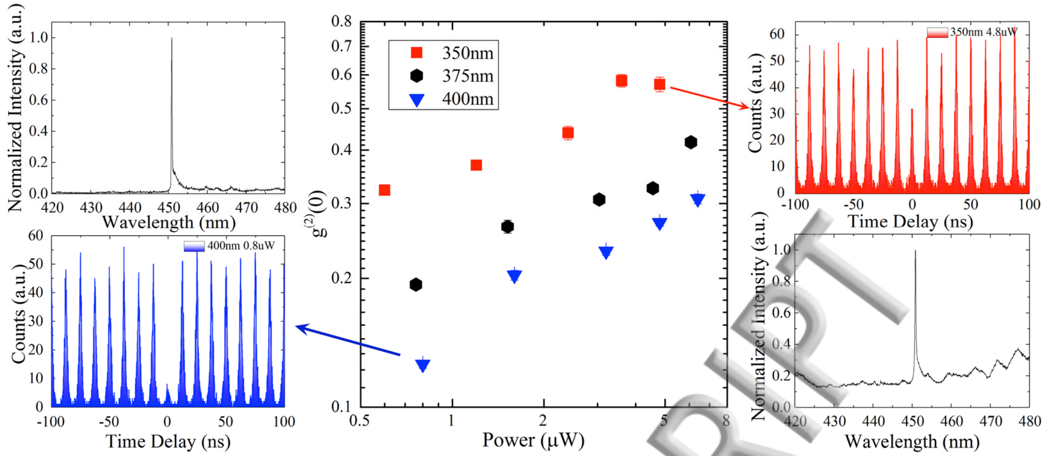

Figure 3. Plot of the measured $g^{(2)}(0)$ values for a range of excitation powers and wavelengths. Also displayed are the autocorrelation histograms and corresponding spectra for the best and worst values of $g^{(2)}(0)$. This corresponds to excitation at 0.8 μW using 400 nm pulsed laser, and 4.8 μW using 350 nm pulsed laser respectively.

We have utilized the recently developed simple one-step porosification and one-step dry etching to form porous micropillars containing InGaN quantum dots. Using these structures, we have explored the impact of excitation conditions on the observed purity of single photon emission from the structures. It has been shown that the value of the autocorrelation $g^{(2)}(0)$ measurement can be greatly reduced by the combination of a low power and low energy excitation laser. In this manner we have obtained a raw (no background correction of any kind) $g^{(2)}(0)$ value of 0.126 ± 0.003.Thus we report a working quantum device utilizing porous GaN. Such a structure is a meaningful step towards the realization of high reliability GaN-based optoelectronics for on-demand single photon sources.

Acknowledgements

This work was supported by the EPSRC (EP/M011682/1), JSPS KAKENHI Grant-in-Aid for Specially Promoted Research (15H05700), KAKENHI project 17K14655, The JSPS Summer Program, and also the Takuetsu program of the Ministry of Education, culture, sports, Science and Technology, Japan.

[1] N. Gisin, G. Ribordy, W. Tittel, and H. Zbinden, Quantum cryptography, *Reviews of modern physics* 74, 145 (2002)

[2] B. Lounis and M. Orrit, Single-photon sources, *Reports on Progress in Physics* 68, 1129 (2005)

[3] P. Kok, W. J. Munro, K. Nemoto, T. C. Ralph, Jonathan P. Dowling, and G. J. Milburn, Linear optical quantum computing with photonic qubits, *Reviews of Modern Physics* 79, 135 (2007).

[4] J. Rarity, P. Owens and P. Tapster, Quantum Random-number Generation and Key Sharing, *Journal of Modern Optics* 41, 2435 (1994)

[5] F. Diedrich and H. Walther, Nonclassical radiation of a single stored ion, *Physical Review Letters* 58, 203 (1987)

[6] B. Lounis and W.E. Moerner, Single photons on demand from a single molecule at room temperature, *Nature* 407, 491 (2000)

[7] A. Kuhn, M. Hennrich, and G. Rempe, Deterministic single-photon source for distributed quantum networking, *Physical Review Letters* 89, 067901 (2002)

[8] C. Kurtsiefer, S. Mayer, P Zarda, and H. Weinfurter, Stable solid-state source of single photons, *Physical Review Letters* 85, 290 (2000)

[9] P. Michler, A. Imamoglu, M.D. Mason, P.J. Carson, G.F. Strouse, S.K. Burrato, Quantum correlation among photons from a single quantum dot at room temperature, *Nature* 406, 968 (2000)

[10] P. Michler, A. Kiraz, C. Becher, W.V. Schoenfeld, P.M. Petroff, L. Zhang, E. Hu, A. Imamoglu, A quantum dot single-photon turnstile device, *Science* 290, 2282 (2000)

[11] S. Nakamura and S.F. Chichibu, *Introduction to nitride semiconductor blue lasers and light emitting diodes*, Taylor and Francis, London, 2000

[12] M. Rau, T. Heindel, S. Unsleber, T. Braun, J. Fischer, S. Frick, S. Nauerth, C. Schneider, G. Vest, S. Reitzenstein, M. Kamp, A. Forchel, S. Höfling, and H. Weinfurter, Free space quantum key distribution over 500 metres using electrically driven quantum dot single-photon sources- a proof of principle experiment, *New Journal of Physics* 16, 0430003 (2014)

[13] S. Deshpande, T. Frost, A. Hazari, P. Battacharya, Electrically pumped single-photon emission at room temperature from a single InGaN/GaN quantum dot, *Applied Physics Letters* 105, 141109 (2014)

[14] T. Wang, T.J. Puchtler, T. Zhu, J.C. Jarman, L.P. Nuttall, R.A. Taylor, Polarisation-controlled single photon emission at high temperatures from InGaN quantum dots, *Nanoscale* 9 (27), 9421 (2017)

[15] M. Holmes, S. Kako, K. Choi, M. Arita, Y, Arakawa, Single photons from a hot solid-state emitter at 350 K, *ACS Photonics*, 3 (4), 543 (2016)

[16] S. Buckley, K Rivoire, J. Vučković, Engineered quantum dot single-photon sources, *Reports on Progress in Physics* 75 126503 (2012)

[17] T. Müller, J. Skiba-Szymanska, A.B. Krysa, J. Huwer, M. Felle, M. Anderson, R.M Stevenson, J, Heffernan, D.A. Richie, A.J. Shields, A quantum light-emitting diode for the standard telecom window around 1,550 nm, *Nature Communications* 9, 862 (2018)

[18] O. Gazzano, S. Michaelis de Vasconcellos, C. Arnold, A. Nowak, E. Galopin, I. Sagnes, L. Lanco, A. Lemaître, P. Senellart, Bright solid-state sources of indistinguishable single photons, *Nature Communications* 4, 1425 (2013)

[19] T. Someya, and Y. Arakawa, Highly reflective GaN/$Al_{0.34}Ga_{0.66}N$ quarter-wave reflectors grown by metal organic chemical vapor deposition, *Applied Physics Letters* 73 (1998)

[20] N. Nakada, H. Ishikawa, T. Egawa, T. Jimbo, M. Umeno, MOCVD growth of high reflective GaN/AlGaN distributed Bragg reflectors, *Journal of Crystal Growth* 237, 961, (2002)

[21] C. Kruse, H. Dartsch, T. Aschenbrenner, S. Figge, D. Hommel, Growth and characterization of nitride-based distributed Bragg reflectors, *Physica Status Solidi B* 248, 1748 (2011)

[22] J.-F. Carlin and M. Ilegems, High-quality AlInN for high index contrast Bragg mirrors lattice matched to GaN, *Applied Physics Letters* 83, 668 (2003)

[23] T. Zhu, Y. Liu, T. Ding, W.Y. Fu, J. Jarman, C.X. Ren, R.V. Kumar, and R.A. Oliver, Wafer-scale fabrication of non-polar mesoporous GaN distributed Bragg reflectors via electrochemical porosification, *Scientific Reports*, 7, 45344 (2017)

[24] R.A. Oliver, G.A.D. Briggs, M.J. Kappers, C.J. Humphreys, S. Yasin, J.H Rice, J.D. Smith, R.A. Taylor, InGaN quantum dots grown by metalorganic vapor phase epitaxy employing a post-growth nitrogen anneal, *Applied Physics Letters* 83, 755 (2003)

[25] T. Zhu, F. Oehler, B.P.L. Reid, R.M. Emery, R.A. Taylor, M.J. Kappers, R.A. Oliver, Non-polar (11-20) InGaN quantum dots with short exciton lifetimes grown by metal-organic vapor phase epitaxy, *Applied Physics Letters* 103, 251905 (2013)

[26] S. Li and A. Waag, GaN based nanorods for solid state lighting, *Journal of Applied Physics* 111, 071101 (2012)

[27] S. Kako, M. Holmes, S. Sergent, M. Bürger, D.J. As, Y. Arakawa, Single-photon emission from cubic GaN quantum dots, *Applied Physics Letters* 104, 011101 (2014)

[28] M. Holmes, S. Kako, K. Choi, M. Arita, Y. Arakawa, Spectral diffusion and its influence on the emission linewidths of site-controlled GaN nanowire quantum dots, Physical Review B 92, 115447 (2015)

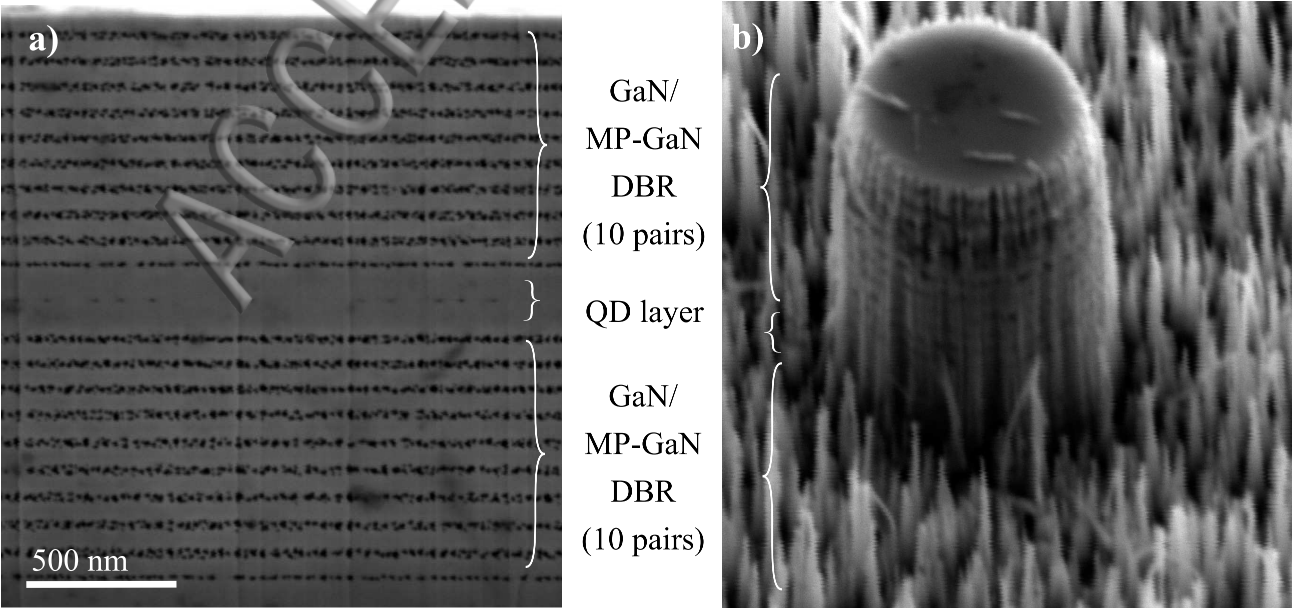
a)
b)
GaN/
MP-GaN
DBR
(10 pairs)
QD layer
GaN/
MP-GaN
DBR
(10 pairs)
500 nm

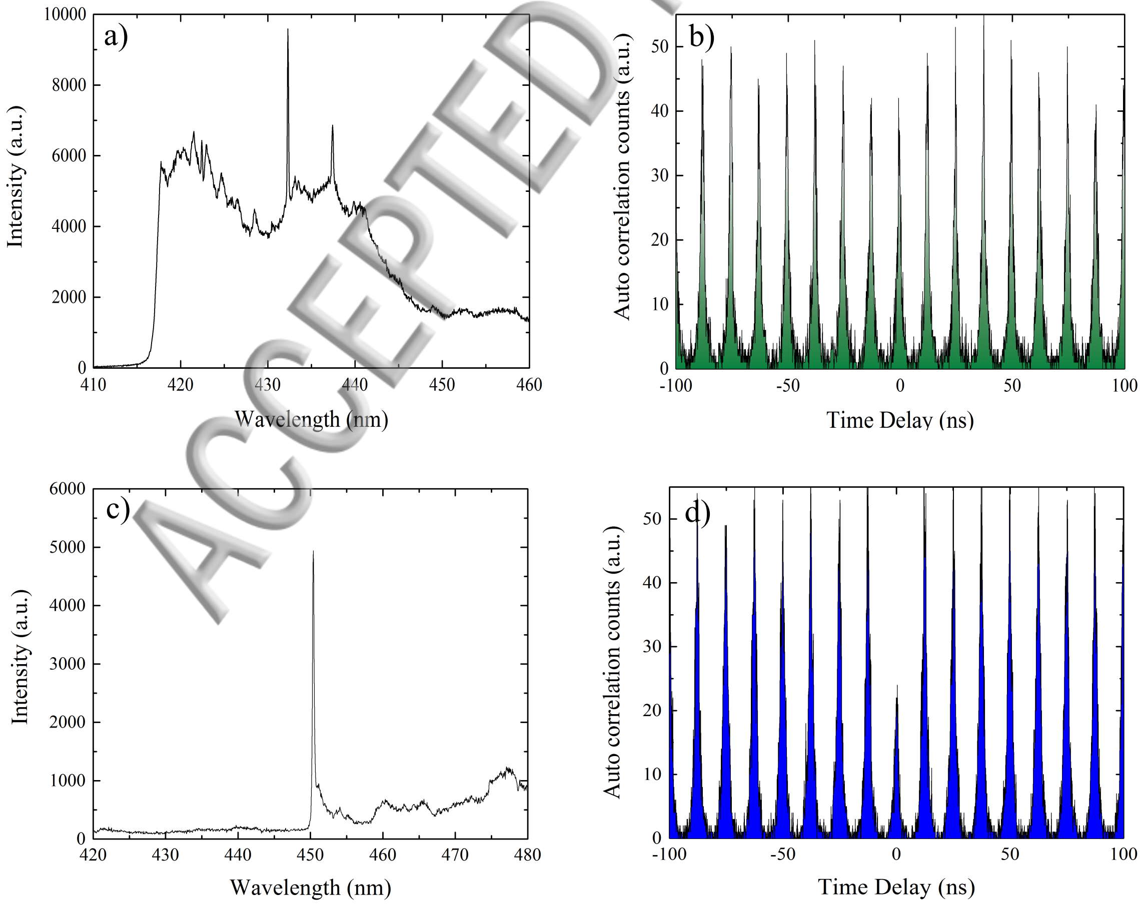

a)
Intensity (a.u.)
Wavelength (nm)
b)
Auto correlation counts (a.u.)
Time Delay (ns)
c)
Intensity (a.u.)
Wavelength (nm)
d)
Auto correlation counts (a.u.)
Time Delay (ns)


Normalized Intensity (a.u.)
1.0
0.8
0.6
0.4
0.2
0.0
420 430 440 450 460 470 480
Wavelength (nm)
400nm 0.8uW
Counts (a.u.)
60 50 40 30 20 10 0
-100 -50 0 50 100
Time Delay (ns)
350nm
375nm
400nm
g$^{(2)}$(0)
0.8 0.7 0.6 0.5 0.4 0.3 0.2 0.1
0.5 1 2 5 8
Power (μW)
350nm 4.8uW
Counts (a.u.)
60 50 40 30 20 10 0
-100 -50 0 50 100
Time Delay (ns)
Normalized Intensity (a.u.)
1.0 0.8 0.6 0.4 0.2 0.0
420 430 440 450 460 470 480
Wavelength (nm)